Journal of Power Sources 196 (2011) 54–61

Contents lists available at ScienceDirect

Journal of Power Sources

journal homepage: www.elsevier.com/locate/jpowsour

Platinum decorated Ru/C: Effects of decorated platinum on catalyst structure and performance for the methanol oxidation reaction

Haili Gao, Shijun Liao, Jianhuang Zeng*, Yichun Xie

School of Chemistry and Chemical Engineering, South China University of Technology, 381 Wushan Road, Tianhe District, Guangzhou 510641, Guangdong, China

ARTICLE INFO

Article history:
Received 18 June 2010
Received in revised form 14 July 2010
Accepted 15 July 2010
Available online 22 July 2010

Keywords:
Catalysts
Platinum decoration
Ruthenium
Methanol oxidation

ABSTRACT

Platinum decorated Ru/C catalysts are prepared by successive reduction of a platinum precursor on preformed Ru/C. Pt:Ru atomic ratios are varied from 0.13:1 to 0.81:1 to investigate the platinum decoration effects on the catalyst's structure and electrochemical performance towards the methanol oxidation reaction (MOR) at room temperature. The catalysts are extensively characterized by X-ray diffraction (XRD), transmission electron microscopy (TEM), and X-ray photoelectron spectroscopy (XPS). Ru@Pt/C catalysts show enhanced mass-normalized activity and specific activity for the MOR relative to Pt/C. For the anodic oxidation of methanol, the ratio of forward to reverse oxidation peak current R (I_f/I_b) varies considerably: R decreases from 5.8 to 0.8 when the Pt:Ru ratio increases from 0.13:1 to 0.81:1. When the ratio of Pt:Ru is 0.42:1, R reaches 0.99 (close to that of Pt/C), and further increase of the Pt:Ru ratio leads to almost no decrease in R. Coincidentally, maximum mass-normalized activity is also obtained when Pt:Ru is 0.42:1.

1. Introduction

Owing to the easy fuel handling/storage, high energy efficiency, and environmental friendliness of direct methanol fuel cells (DMFCs), great attention has been paid to their development over the past decade [1].

DMFCs have great potential applications in small portable electronic devices, such as third-generation mobile telephones, laptops, and personal digital assistants. The ever-growing markets for portable devices has in turn prompted and advanced the rapid development of DMFCs. Unfortunately, the performance of the anode electrocatalysts is still unsatisfactory. Pt or Pt-based nanoparticles have been the targeted electrocatalysts, and intensive studies have been made to enhance their catalytic activities [2–5]. Aside from its use in electrocatalysts, Pt is in demand for numerous other applications, including catalytic converters for air pollution control in vehicles, a growing jewellery market, catalysts for various purposes (especially petroleum and chemicals processing). Therefore, Pt-only catalysts are very costly, especially those with high loadings.

In order to promote the commercialization of DMFCs, further improvements are still required to enhance catalytic activity for the methanol oxidation reaction and to significantly lower Pt content. An efficient way to decrease the loadings of Pt and other precious metals and thereby make the most efficient use of them is by better dispersion of the metal either through the use of high surface area supports or the construction of special structures [6]. Core–shell construction has been proven to be an effective mean to increase the utilization efficiency of precious metal electrocatalysts (as the shell) and to enhance electrocatalytic activity accordingly [7,8]. Over the past few years, a number of investigations into core–shell structured nanoparticles as fuel cell catalysts have been conducted and encouraging results obtained [9–11].

It has been generally recognized that Pt–Ru bimetallic catalysts are the most promising anode materials for DMFCs, since ruthenium is favorable for removing the adsorbed CO intermediates from Pt, which are formed during methanol oxidation and thus poison the catalysts, reducing their activity for the MOR [3,12].

In addition, the price of Ru is about one-seventh that of platinum, according to current online prices for noble metals, and Ru is more stable than other base metals (e.g., Fe, Co, and Ni). Based on these understandings, preparation of Ru@Pt/C catalysts has been receiving ever-increasing attention. Sasaki et al. [13] developed electrocatalysts with monolayer-level Pt content by depositing Pt on the surfaces of Ru nanoparticles through galvanic replacement of Cu adlayers. Compared with a commercial PtRu/C alloy catalyst, the electrocatalyst with a monolayer of Pt (Pt_{ML}/Ru/C) showed three times higher Pt mass activity, as well as improved durability for methanol oxidation. Alayoglu et al. [14] prepared Ru@Pt/C electrocatalyst and their extensive experimental results showed that the electrocatalyst has high performance for oxidizing CO in H_2. Chen et al. [15] prepared Pt decorated Ru nanoparticles with low Pt content

* Corresponding author. Tel.: +86 20 8711 3586; fax: +86 20 8711 3586.
E-mail address: cejhzeng@scut.edu.cn (J. Zeng).

0378-7753/$ – see front matter © 2010 Elsevier B.V. All rights reserved.
doi:10.1016/j.jpowsour.2010.07.040

by a redox–transmetalation process and found that the catalyst had higher activity toward methanol oxidation than commercial Pt–Ru black catalyst. Therefore, it can be concluded that Ru@Pt electrocatalysts are good candidates for the MOR, and it is worth conducting detailed experiments to determine the optimum Pt:Ru ratio and amount of Pt.

In the present work, core–shell Ru@Pt/C catalysts were synthesized by a two-stage route. The Pt shell amount on the Ru nanoparticles was achieved by varying the molar ratios of Pt:Ru. Various techniques were used to characterize the formation of Ru–Pt core–shell nanoparticles, including transmission electron microscopy (TEM), X-ray diffraction (XRD), and X-ray photoelectron spectroscopy (XPS). The effects of the Pt:Ru atomic ratio on catalytic activity for the MOR were examined by cyclic voltammetry. Catalytic activity enhancement was inferred from the suppression of CO intermediate formation on the catalysts.

2. Experimental

2.1. Catalyst preparation

Ru/C, the carbon-supported Ru core, was prepared by an impregnation-reduction method. 300 mg pretreated carbon black (Cabot Corp., BET: 237 $m^2\,g^{-1}$, denoted as C) was mixed with 207 mg $RuCl_3{\cdot}3H_2O$ in diluted HCl solution to prepare impregnated Ru/C. The mixture was ultrasonically blended for 30 min and then magnetically stirred at 70 °C to allow water evaporation. The black powder was then placed in a ceramic boat and heated in a tubular furnace under flowing H_2 at 200 °C for 2 h.

Ru@Pt/C catalysts (ratios of Pt:Ru = 0.13:1, 0.22:1, 0.35:1, 0.42:1; 0.55:1; 0.61:1, and 0.81:1) were prepared by an organic colloid method [16]. It is to be noted that the notation Ru@Pt does not necessarily mean a perfect core–shell structure hereafter. Calculated amounts of hexachloroplatinic acid ($H_2PtCl_6{\cdot}6H_2O$) and sodium citrate (with a 2.5:1 molar ratio of sodium citrate to hexachloroplatinic acid) were dissolved in 15 ml ethylene glycol (EG) and then stirred for 30 min to entirely dissolve the sodium citrate. Afterwards, as-prepared Ru/C was added to the mixture, followed by adjustment of the pH to greater than 10 by the drop-wise addition of 5 wt.% KOH/EG solution under vigorous stirring. The mixture was then transferred into a Teflon-lined autoclave and conditioned at 120 °C for 6 h, followed by filtering, washing, and vacuum drying at 70 °C. Therefore, in addition to 20 wt.% Ru in the Ru@Pt/C catalyst, the exact Pt content for Ru@Pt/C with Pt:Ru ratios of 0.13:1, 0.22:1, 0.35:1, 0.42:1; 0.55:1; 0.61:1, and 0.81:1 was 5, 8, 13, 16, 21, 23, and 31 wt.%, respectively. For a fair comparison, 20 wt.% Pt/C was prepared following a similar procedure, except that XC-72 carbon was added instead of Ru/C.

2.2. Materials characterization

X-ray powder diffractions (XRD) were carried out on a Shimadzu XD-3A (Japan) using filtered Cu Kα radiation. The 2θ angular region between 20° and 80° was explored at a scan rate of 4° min^{-1}. The surface morphologies of the catalysts were studied via a transmission electron microscope (JEOL JEM-2010HR, Japan) operated at 200 kV. The X-ray photoelectron spectroscopy (XPS) measurement was carried out in an ultrahigh vacuum on a PerkinElmer PHI1600 system (PerkinElmer, USA) using a single Mg Kα X-ray source operating at 300 W and 15 kV. The binding energies (BEs) were calibrated using the C 1s peak of graphite at 284.5 eV as the reference.

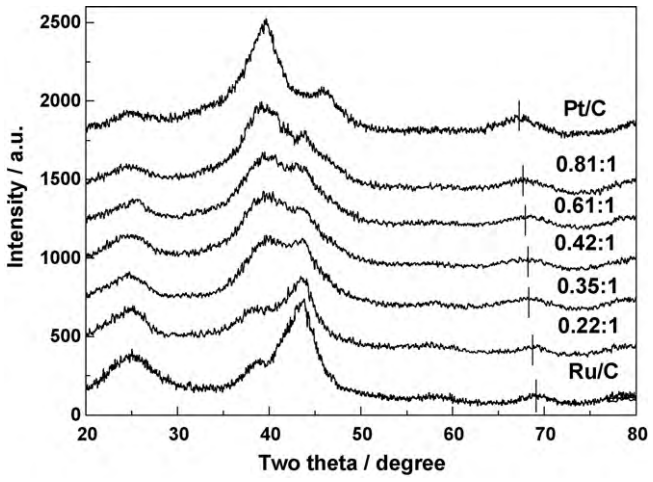

Fig. 1. X-ray diffraction patterns of Ru/C, Ru@Pt/C with different atomic ratios of Pt to Ru and Pt/C.

2.3. Electrochemical measurements

Electrochemical measurements were carried out on an electrochemical work station (Ivium, Netherlands) at room temperature, using a standard three-electrode electrochemical cell. A platinum wire and an Ag/AgCl (saturated KCl) electrode were used as counter and reference electrode, respectively. The catalyst layer on the glassy carbon electrode (5 mm diameter) was prepared as follows: 5 mg catalyst was dispersed ultrasonically in 1 ml Nafion/ethanol (0.25 wt.% Nafion) for 30 min. Then 6 μl ink was pipetted and spread on the glassy carbon surface, and the electrode was dried in air to obtain a thin catalyst layer. Cyclic voltammetry (CV) was performed in 0.50 M H_2SO_4 for the electrochemical surface area (ECSA) measurements and in 0.50 M H_2SO_4 + 0.50 M CH_3OH solution for the oxidation of methanol, at a scan rate of 30 mV s^{-1}. For ECSA measurements, the solutions were purged with N_2 for 20 min prior to each experiment.

3. Results and discussion

Fig. 1 shows the XRD patterns of Ru@Pt/C catalysts with different Pt:Ru ratios; Ru/C and Pt/C catalyst are included for comparison. The broad reflection peak observed at ca. 25° in all the XRD patterns is due to the graphitic nature of the carbon support. All the catalysts show reflection peaks at 39.8° and 44.0°, which correspond to Pt(1 1 1) and Ru(1 0 1). This implies that Pt was not alloyed with Ru. Interestingly, the reflection peak at ca. 68.0° shifted to lower angles and the reflection peak intensity of Pt(1 1 1) became stronger as Pt content increased, indicating that as the Pt:Ru ratio increased, more Pt atoms covered the surfaces of Ru particles.

The average particle sizes of the catalysts were evaluated by Jada software (supplied by the XRD vendor) based on the Pt(2 2 0) peak, and presented in Table 1. It can be seen that particle size increased with Pt content, which may serve as evidence of Pt covering Ru nanoparticles. It should be noted that due to the poor resolution of

Table 1
The average particle sizes of the catalysts calculated from XRD.

Pt/Ru atomic ratio	0.13	0.22	0.35	0.42	0.55	0.61	0.81
Particle size (nm)	2.6	2.6	2.8	2.9	3.0	3.2	3.5

the XRD patterns, the particle sizes read from the Jada software can only be used as a rough reference.

TEM images with different magnifications were obtained to get more information about Ru@Pt particle size and size distribution. Fig. 2 shows the TEM images of Ru/C (A and B), Ru@Pt/C catalysts with different molar ratios (C–F), Pt/C (G and H), and the corresponding particle size distributions. It can be observed that the particles were highly dispersed on the carbon support and had a narrow size distribution. By counting more than 100 particles in images B, D, F, and H, the average particle sizes were determined to be 2.6, 2.9, 3.1, and 2.8 nm for Ru/C, Ru@Pt/C (Pt:Ru = 0.35), Ru@Pt/C (Pt:Ru = 0.55), and Pt/C, respectively, which were in fairly good agreement with the XRD observations. Due to the limited resolution, it is difficult to observe the core–shell structure of Ru@Pt/C.

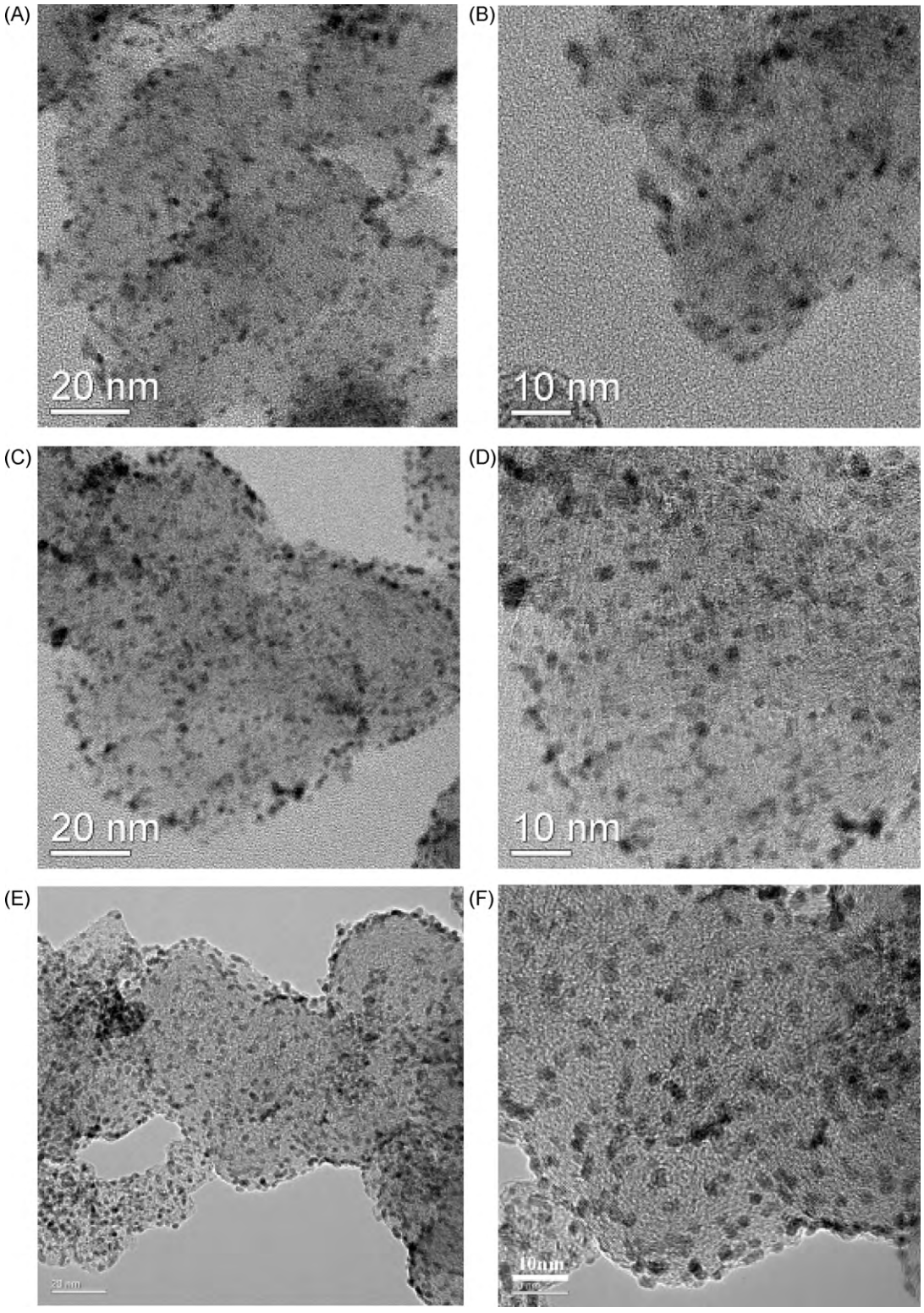

Fig. 2. TEM images of Ru/C (A and B), Ru@Pt/C with atomic ratio Pt:Ru = 0.35 (C and D), Pt:Ru = 0.55 (E and F), Pt/C (G and H) and the corresponding particle size distribution of Ru/C (I), Ru@Pt/C (Pt/Ru atomic ratio = 0.35) (J) and Ru@Pt/C (Pt/Ru atomic ratio = 0.55) (K).

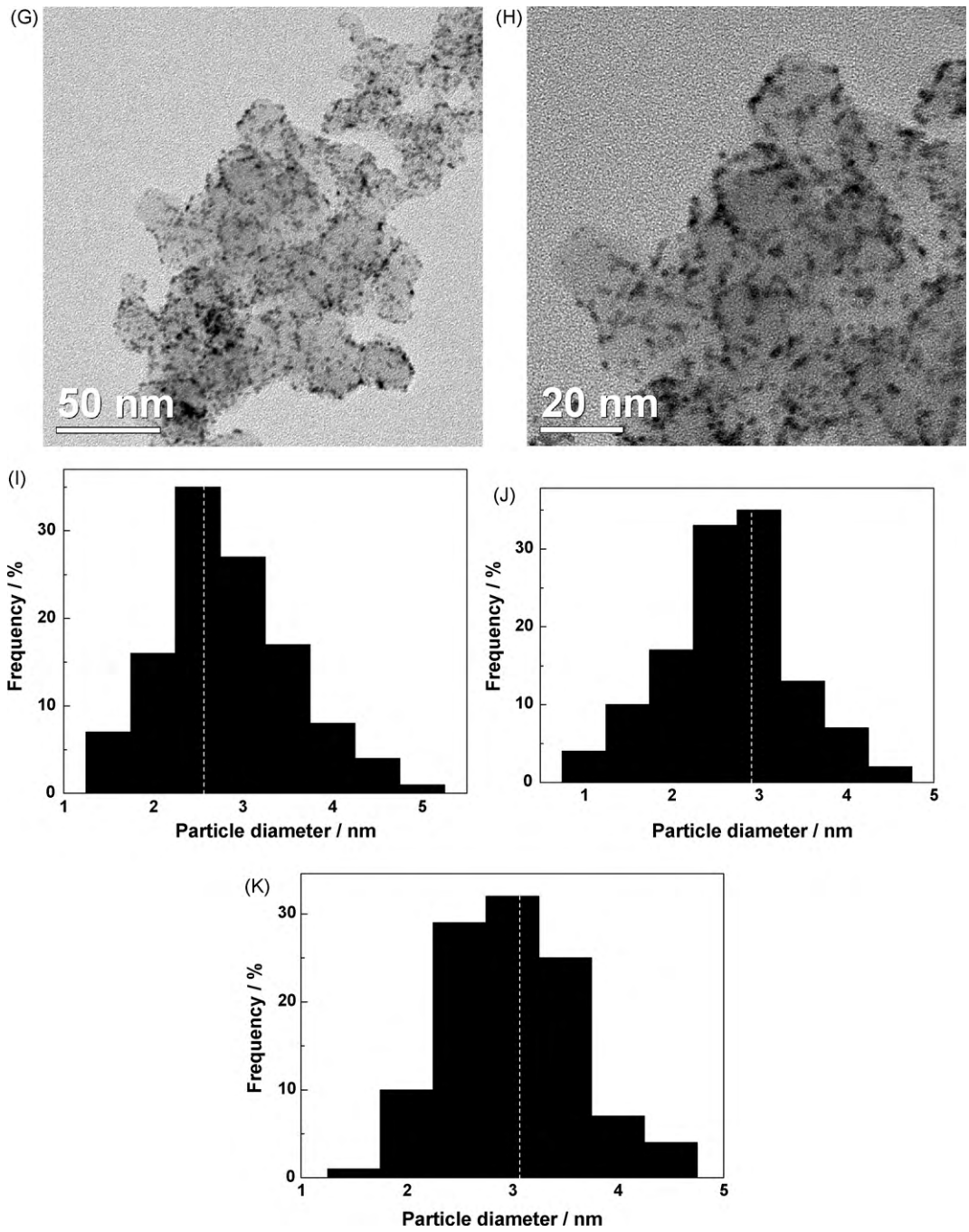

Fig. 2. (*Continued*).

The particle growth of Ru@Pt relative to Ru nanoparticles may be understood as follows: Pt nucleation probably occurred preferentially on the pre-formed Ru nanoparticles by the reaction of adsorbed $PtCl_6^{2-}$anions with the reducing agent [17,18]. Formation of isolated Pt nanoparticles on the carbon support of Ru/C (rather than on the Ru nanoparticles) is certainly inevitable, but less likely because the creation of new nuclei is not energetically favorable in the solution phase [19]. The increase in particle size could serve as indirect evidence for the growth of Pt on the Ru surface.

X-ray photoelectron spectroscopy was further carried out on the catalysts to obtain information about surface composition and electronic properties. The detected atomic ratio of Pt to Ru for Ru@Pt/C catalysts with Pt:Ru ratios of 0.26:1, 0.42:1, and 0.55:1 were ca. 0.25:1, 0.45:1, and 0.78:1, respectively. It can be seen that when the feed Pt:Ru ratio was low (0.26:1 and 0.42:1), the detected Pt:Ru ratio was close to the feed ratio. As the feed ratio increased to 0.55:1, the detected ratio increased to 0.78:1, indicative of Pt-enriched surfaces.

The Pt 4f spectra of the catalysts are shown in Fig. 3(A–D). The Pt 4f signal in all samples can be deconvoluted into two doublets. For Pt-only catalysts (Fig. 3D), the peaks with binding energies of 71.3 and 74.5 eV are ascribed to metallic Pt [20,21], whereas the peaks corresponding to 72.3 and 76.5 eV can be assigned to Pt(II) species in the form of $Pt(OH)_2$ or PtO [22].

The metallic Pt $4f_{7/2}$ lines for Ru@Pt/C (0.55:1), Ru@Pt/C (0.42:1), and Ru@Pt/C (0.26:1) occurred at 71.5, 71.8, and 72.1 eV, respectively, whereas the metallic Pt $4f_{5/2}$ lines were at 74.7, 75.0, and

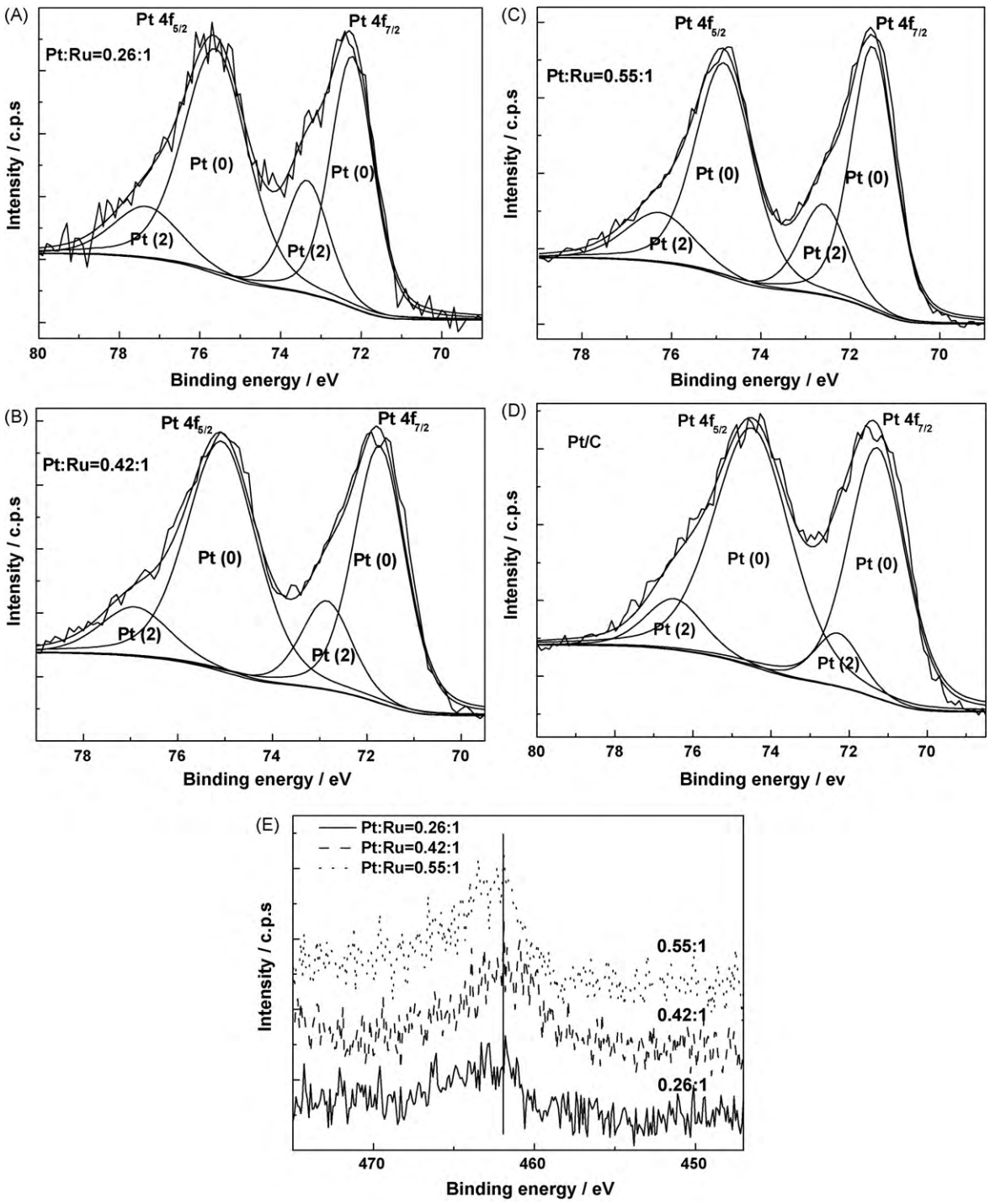

Fig. 3. XPS spectra of Pt 4f (A–D) and Ru 3p (E) of the catalysts.

75.6 eV, respectively. The Pt binding energies of all Ru@Pt/C catalysts were higher than that of Pt/C. Similar results have been reported by Alayoglu et al. [14]. The percentage of Pt in the zero valent state for Ru@Pt/C (0.26:1), Ru@Pt/C (0.42:1), and Ru@Pt/C (0.55:1) was 75.1%, 79.0%, and 77.9%, respectively, similar to that in Pt/C (78.0%). It can be concluded that the existence of ruthenium underlay did not change the oxidation states of the decorating platinum.

The Ru 3p spectra in Fig. 3E were laden with much noise and poorly resolved, making it difficult to quantify the BE states of Ru. However, the Ru in the Ru@Pt/C catalysts can still be clearly identified.

Fig. 4 shows the CV results of Pt/C and Ru@Pt/C catalysts with different Pt:Ru ratios in 0.50 M H_2SO_4 solution. It can be observed that the intensity of the H_2 desorption peak increased with Pt content. Ignoring the adsorption of hydrogen on Ru, the number of Pt surface atoms was estimated from the charge associated with hydrogen desorption in the region of −0.20 to 0.11 V, using the stoichiometry of one adsorbed H atom per Pt atom. The ECSA in $m^2\ g^{-1}$ was then calculated, assuming a correspondence value of 0.21 mC cm^{-2} Pt [23]. The ECSA of Pt/C was calculated to be 67.5 $m^2\ g^{-1}$ Pt. From Fig. 4K it can be observed that the ECSAs increased with the Pt:Ru ratio, then decreased when the maximum ECSA (121.5 $m^2\ g^{-1}$) was reached at Pt:Ru = 0.42. This increase in ECSAs was attributed to

the initial rise in relative Pt content when Pt:Ru was lower than 0.42. It is probable that complete coverage of the Ru core was reached when the Pt:Ru ratio was 0.42, and additional increases in Pt content only led to thicker Pt shells, with consequently decreased ECSAs. That the ECSA of Ru@Pt/C was higher than that of Pt/C might also indicate the former's higher Pt utilization efficiency, which would be further indirect evidence for the core–shell structure of Ru@Pt/C.

Fig. 5 shows the CVs of Ru@Pt/C catalysts with different Pt:Ru ratios in 0.50 M H_2SO_4 + 0.50 M CH_3OH at room temperature, by both the geometric electrode surface area and the Pt mass in the catalysts. The onset potentials of Ru@Pt/C for methanol oxidation with Pt:Ru ratios of 0.13:1, 0.26:1, 0.42:1, 0.61:1, and 0.81:1 are 0.12, 0.13, 0.12, 0.14, and 0.16 V, which are negatively shifted compared with that of Pt/C (0.17 V). It can be observed that as the Pt:Ru ratio increased, the activities normalized by the geometric electrode surface area for the MOR also increased (Fig. 5A); this trend is most clearly evident in Fig. 5C. These results are undoubtedly due to the MOR taking place at the active sites of Pt, and the increasing Pt/Ru ratio providing more of these active sites. The mass-normalized activity in Fig. 5B initially increased with Pt loading, then gradually decreased, an indication of optimum Pt utilization efficiency when the Pt:Ru ratio reached 0.42. A similar phenomenon has been observed by Li et al. [24] and Zhu et al. [25] during electrocatalytic reduction of oxygen on Au@Pt and ethanol oxidation on Au@Pd/C catalysts, respectively. In addition to mass activity (in terms of

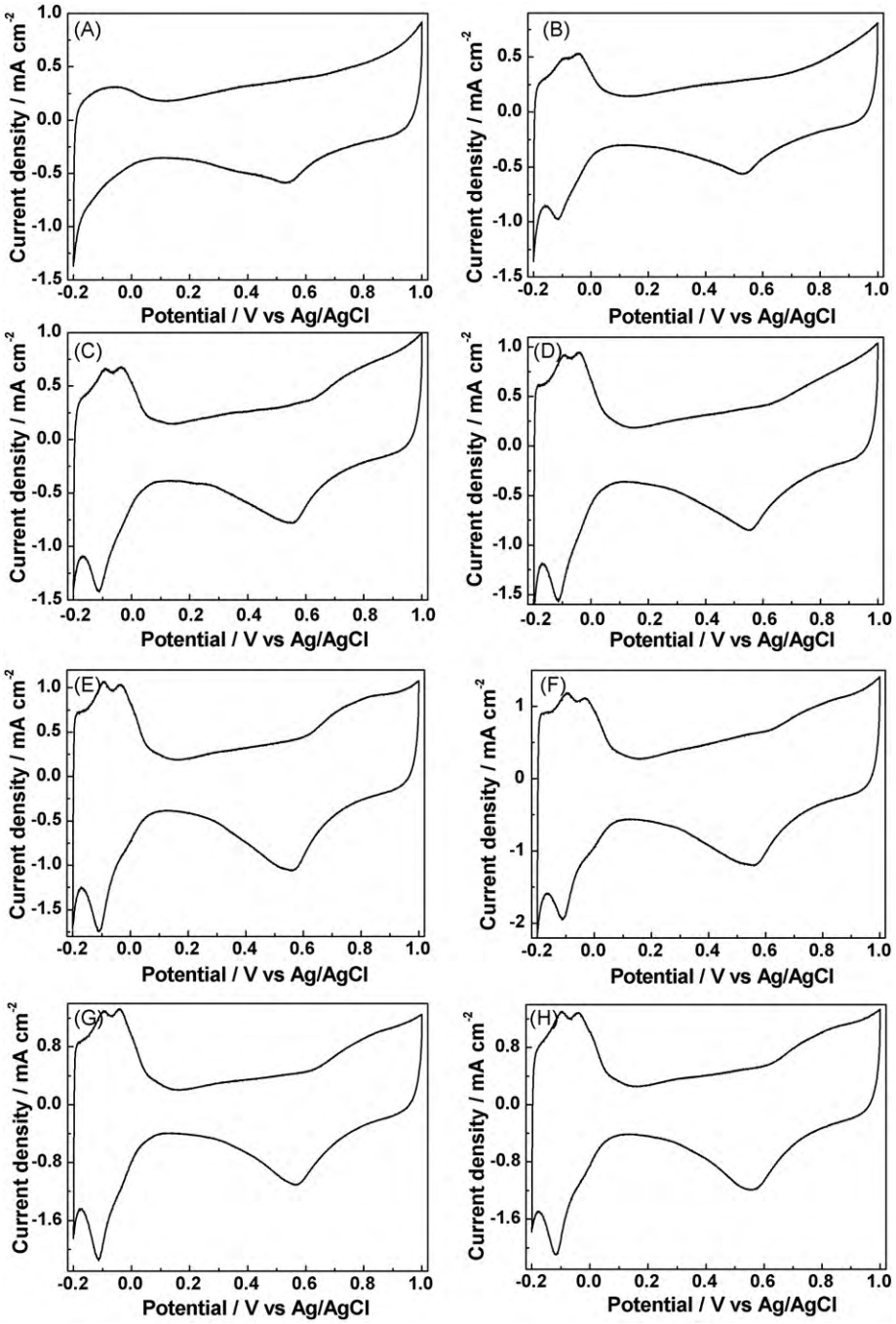

Fig. 4. Cyclic voltammograms of Ru@Pt/C catalysts with different atomic ratios of Pt to Ru: (A) 0.13, (B) 0.22, (C) 0.26, (D) 0.35, (E) 0.42, (F) 0.49, (G) 0.55, (H) 0.61, (I) 0.81 and Pt/C (J) in 0.50 M H_2SO_4 solution (room temperature, scanning rate of 30 mV s^{-1}) and ECSAs calculated from the hydrogen desorption area (K).

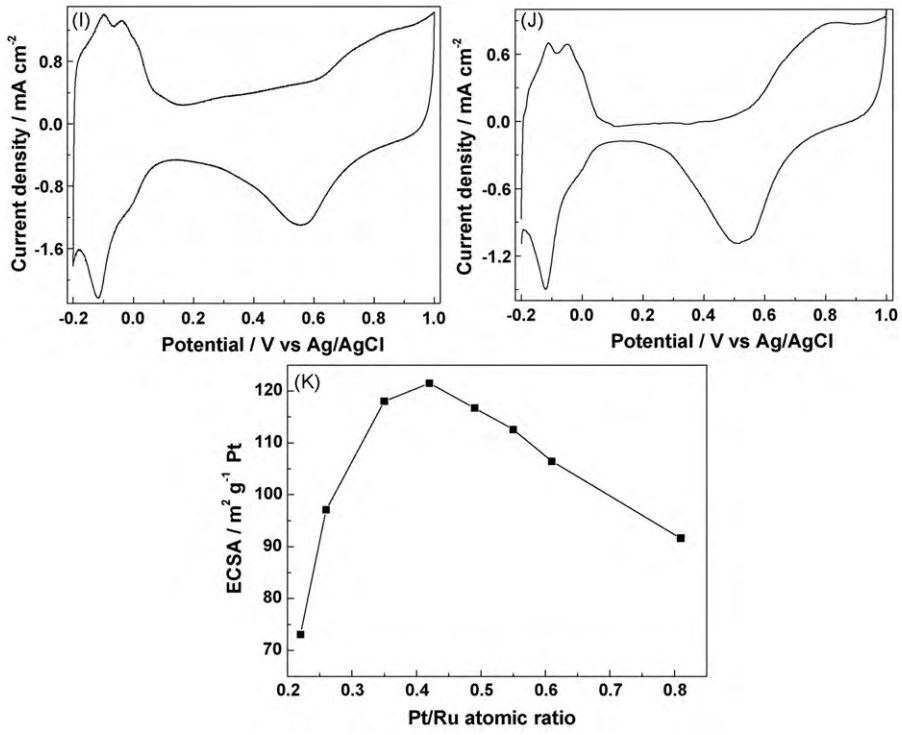

Fig. 4. (*Continued*).

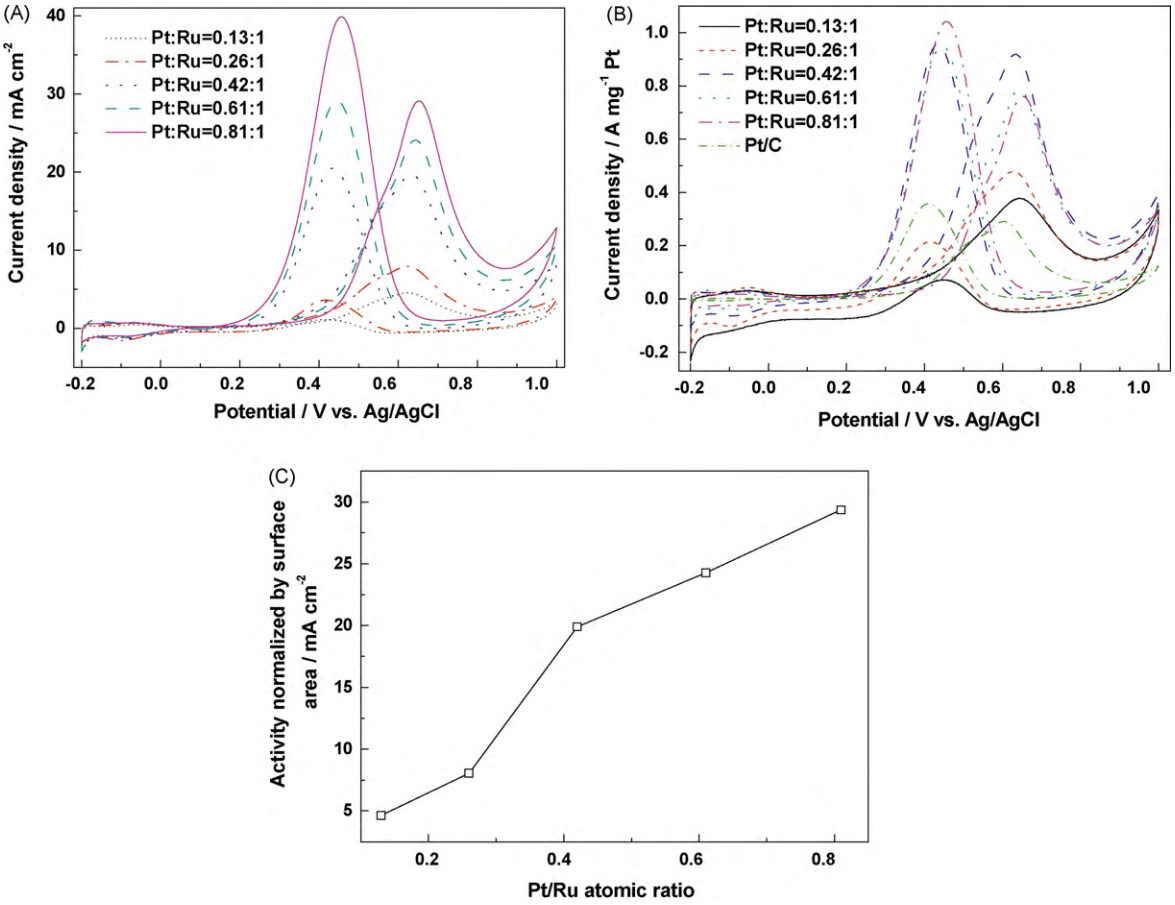

Fig. 5. Cyclic voltammograms of Ru@Pt/C catalysts with different atomic ratios of Pt to Ru (0.13, 0.26, 0.42, 0.61 and 0.81) in 0.50 M H_2SO_4 + 0.50 M CH_3OH (room temperature, scanning rate of 30 mV s^{-1}): (A) normalized by the geometric electrode surface, (B) normalized by the Pt mass in the catalysts and (C) changes of geometric surface area normalized activity with varying Pt/Ru atomic ratio.

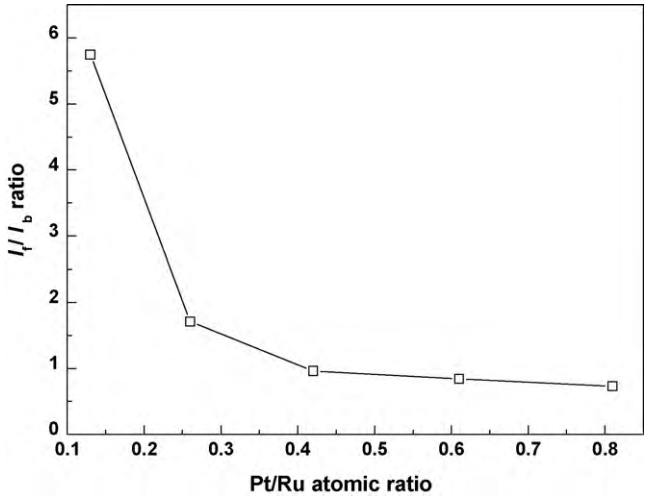

Fig. 6. Changes of Pt/Ru atomic ratio with I_f/I_b value.

activity normalized by geometric surface area and Pt mass loadings), specific activity, which is normalized by ECSA, refers to the intrinsic activity of the catalysts. The specific activity of Ru@Pt/C with ratios of 0.26:1, 0.42:1, 0.61:1, and 0.81:1 was 4.9, 7.6, 7.4, and 8.3 A cm^{-2}, respectively, significantly higher than that of Pt/C (2.6 A cm^{-2}).

The change in I_f/I_b value (defined as the ratio between the forward and backward current densities) with the change in Pt:Ru ratio is given in Fig. 6. The forward peak current density (I_f) is generally regarded as methanol oxidation on non-poisoned catalysts, while the backward peak current density (I_b) is associated with methanol oxidation on regenerated catalysts (after the removal of the carbonaceous intermediate) [26]. The ratio of forward to backward peak current can be used to evaluate the CO tolerance of catalysts [27,28]. Generally, a higher I_f/I_b ratio implies higher CO tolerance. From Fig. 6 it can be seen that I_f/I_b decreased sharply as the Pt:Ru atomic ratio increased at the beginning, and reached a plateau when Pt:Ru was 0.42:1. When the Pt:Ru atomic ratio was 0.13, the I_f/I_b value was as high as 5.75, indicating the highest CO tolerance. The I_f/I_b value decreased as fewer Ru particles became available when the Pt:Ru ratio increased. When Pt:Ru reached 0.42 the I_f/I_b value was 0.99, very close to that of Pt/C (0.81), indicating an Ru surface almost fully covered by Pt. Coincidentally, the mass-normalized activity of Ru@Pt/C with Pt:Ru = 0.42:1 was also the highest amongst the catalysts.

4. Conclusions

A series of Ru@Pt/C catalysts have been successfully prepared by a two-step method based on pre-formed Ru/C. XRD and TEM observations clearly showed the particle growth of Ru@Pt/C relative to Ru/C, which may indicate the successful decoration of Ru with Pt. While the Pt oxidation states of Ru@Pt/C were unchanged, the binding energy of Pt(0) shifted to high values compared with that of Pt/C. Electrochemical measurements using cyclic voltammetry showed that the Ru@Pt/C displayed enhanced mass-normalized and specific activity relative to Pt/C. The I_f/I_b value of Ru@Pt/C was also higher than that of Pt/C, indicating enhanced CO tolerance. This study's decoration of pre-formed Ru/C by a Pt shell has thus proven to be an effective way for constructing highly active DMFC anode catalysts.

Acknowledgments

We would like to thank the National Scientific Foundation of China (NSFC Project Nos. 20673040 and 20876062), the Ministry of Science and Technology of China (Project No. 86309), and the Fundamental Research Funds for the Central Universities (SCUT) for financial support of this work.

References

[1] H. Zhao, L. Li, J. Yang, Y. Zhang, Electrochem. Commun. 10 (2008) 1527.
[2] X.Z. Fu, Y. Liang, S.P. Chen, J.D. Lin, D.W. Liao, Catal. Commun. 10 (2009) 1893.
[3] L. Li, Y. Xing, J. Phys. Chem. C 111 (2007) 2803.
[4] G. Selvarani, S.V. Selvaganesh, S. Krishnamurthy, G.V.M. Kiruthika, P. Sridhar, S. Pitchumani, A.K. Shukla, J. Phys. Chem. C 113 (2009) 7461.
[5] C. Paoletti, A. Cemmi, L. Giorgi, R. Giorgi, L. Pilloni, E. Serra, M. Pasquali, J. Power Sources 183 (2008) 84.
[6] T. Matsumoto, T. Komatsu, K. Arai, T. Yamazaki, M. Kijima, H. Shimizu, Y. Takasawa, J. Nakamura, Chem. Commun. 7 (2004) 840.
[7] Z. Liu, G.S. Jackson, B.W. Eichhorn, Angew. Chem. Int. Ed. 49 (2010) 3173.
[8] T. Ghosh, M.B. Vukmirovic, F.J. DiSalvo, R.R. Adzic, J. Am. Chem. Soc. 132 (2010) 906.
[9] I. Srnová-Šloufová, F. Lednický, A. Gemperle, J. Gemperlová, Langmuir 16 (2000) 9928.
[10] A. Henglein, J. Phys. Chem. B 104 (2000) 2201.
[11] H. Wang, C. Xu, F. Cheng, M. Zhang, S. Wang, S.P. Jiang, Electrochem. Commun. 10 (2008) 1575.
[12] H.C. Cha, C.Y. Chen, J.Y. Shiu, J. Power Sources 192 (2009) 451.
[13] K. Sasaki, R.R. Adzic, J. Electrochem. Soc. 155 (2008) B180.
[14] S. Alayoglu, A.U. Nilekar, M. Mavrikakis, B. Eichhorn, Nat. Mater. 7 (2008) 333.
[15] C.H. Chen, L.S. Sarma, D.Y. Wang, F.J. Lai, C.C. Al Andra, S.H. Chang, D.G. Liu, C.C. Chen, J.F. Lee, B.J. Hwang, Chem. Catal. Chem. 2 (2010) 159.
[16] S. Liao, K.A. Holmes, H. Tsaprailis, V.I. Birss, J. Am. Chem. Soc. 128 (2006) 3504.
[17] R. Wang, H. Li, H. Feng, H. Wang, Z. Lei, J. Power Sources 195 (2010) 1099.
[18] W. Wang, R. Wang, S. Ji, H. Feng, H. Wang, Z. Lei, J. Power Sources 195 (2010) 3498.
[19] J. Zeng, J.Y. Lee, W. Zhou, J. Power Sources 159 (2006) 509.
[20] R. Chetty, S. Kundu, W. Xia, M. Bron, W. Schuhmann, V. Chirila, W. Brandl, T. Reinecke, M. Muhler, Electrochim. Acta 54 (2009) 4208.
[21] R.J.K. Wiltshire, C.R. King, A. Rose, P.P. Wells, H. Davies, M.P. Hogarth, D. Thompsett, B. Theobald, F.W. Mosselmans, M. Roberts, A.E. Russell, Phys. Chem. Chem. Phys. 11 (2009) 2305.
[22] A.S. Aricò, P.L. Antonucci, E. Modica, V. Baglio, H. Kim, V. Antonucci, Electrochim. Acta 47 (2002) 3723.
[23] Y.K. Zhou, B.L. He, W.J. Zhou, J. Huang, X.H. Li, B. Wu, H.L. Li, Electrochim. Acta 49 (2004) 257.
[24] X. Li, J. Liu, W. He, Q. Huang, H. Yang, J. Colloid Interf. Sci. 344 (2010) 132.
[25] L.D. Zhu, T.S. Zhao, J.B. Xu, Z.X. Liang, J. Power Sources 187 (2009) 80.
[26] J. Prabhuram, R. Manoharan, J. Power Sources 74 (1998) 54.
[27] Z. Liu, X.Y. Ling, X. Su, J.Y. Lee, J. Phys. Chem. B 108 (2004) 8234.
[28] T. Maiyalagan, J. Solid State Electrochem. 13 (2009) 1561.